Observation of Arc Trails with Significant Damage due to Glow Discharge Wall Conditioning in the Large Helical Device

Yuki HAYASHI[1)], Suguru MASUZAKI[1)], Gen MOTOJIMA[1,2)], Dogyun HWANGBO[3)], Yutaka FUJIWARA[1)], Mingzhong ZHAO[1)] and the LHD Experiment Group[1)]

[1)]*National Institute for Fusion Science, National Institutes of Natural Sciences, Toki 509-5292, Japan*
[2)]*The Graduate University for Advanced Studies, SOKENDAI, Toki 509-5292, Japan*
[3)]*Faculty of Pure and Applied Sciences, University of Tsukuba, Tsukuba 305-8577, Japan*

(Received 2 December 2020 / Accepted 1 March 2021)

We report the observation of arcing damage on the diagnostic shutter during the glow discharge wall conditioning in LHD. The diagnostic system has no experience of plasma discharge produced by electron or ion cyclotron resonance heating or neutral beam injection. The arc trails were observed on the aluminum surface but not on the stainless steel although both materials were exposed to the glow discharge with the same duration. The difference in work functions between two materials may be a cause to divide the conditions of arcing ignition.

© *2021 The Japan Society of Plasma Science and Nuclear Fusion Research*

Keywords: glow discharge conditioning, arcing, LHD

DOI: 10.1585/pfr.16.1202061

Glow discharge conditioning (GDC) is an essential wall conditioning technique in tokamaks and stellarators to produce high performance plasma [1]. Physical or chemical sputtering by impacts of accelerated ions release impurities absorbed in the material. On the other hand, the degradation of the optical properties of the diagnostic mirror due to the GDC was speculated in Large Helical Device (LHD) [2]. Further, arc trails were inspected in non-plasma irradiation region in Wendelstein 7-X (W7-X) [3], where the arcing seemed to be initiated in GDC because of there being no linearity in the trails. This Rapid Communication presents the observation of arc trails with large area on the diagnostic system, which was installed during a brief GDC in LHD.

Figures 1 (a) and (b) show the pictures of the shutter for the mirror of Fast-Ion D Alpha (FIDA) diagnostic system [4] before and after the GDC. Serious damages due to the many arc trails on the shutter surface made of aluminum (Al) were clearly observed. Figures 1 (d) and (e) show the pictures of the shaft for gating the shutter. After the GDC (see Fig. 1 (e)), a number of arc trails covered the most part of the Al area in common with the shutter surface in Fig. 1 (b). On the other hand, a part of the diagnostic system made of stainless steel (SS) survived the arcing damage.

Figure 2 shows a top view of the LHD vacuum vessel. Many arc trails were observed on the shutter surface located at the outboard side of the toroidal section #7. In the LHD GDC, in-vessel components including first walls and divertor plates are grounded and represent the discharge cathode. The shutter and shaft for FIDA diagnostic are also

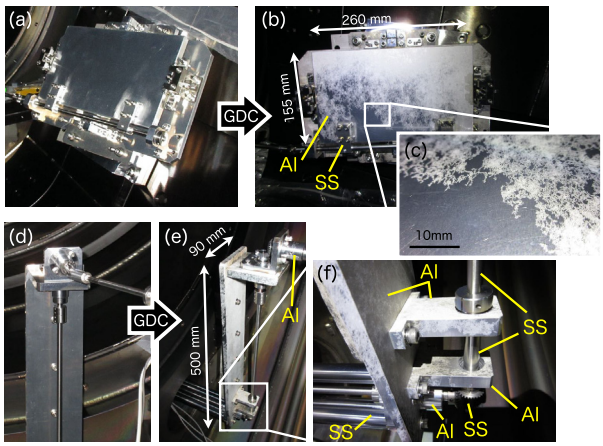

Fig. 1 Pictures of the shutter (a) before and (b) after the GDC and driving shaft (d) before and (e) after the GDC. (c) and (f) are enlarged pictures of (b) and (e), respectively.

grounded. The secondary electron emissions due to ion impact with the plasma facing wall sustains the weakly ionized GDC plasma. The electron impact ionization with the neutral gas produces the ions which are accelerated toward the surface in the potential fall. The GDC is maintained by a steady state DC current between the cathode and two anodes at the top ports of sections #4.5 and #10.5. Multiple anodes distributed in a toroidal direction contribute to homogeneous discharge over the vacuum vessel. Ne and H_2 gases are injected from the bottom port at section #3.5 for keeping the neutral pressure in the vessel to be ~1 Pa. The sputtered impurity particles are pumped out by two turbomolecular pumps at section #7.

author's e-mail: hayashi.yuki@nifs.ac.jp

© 2021 The Japan Society of Plasma Science and Nuclear Fusion Research

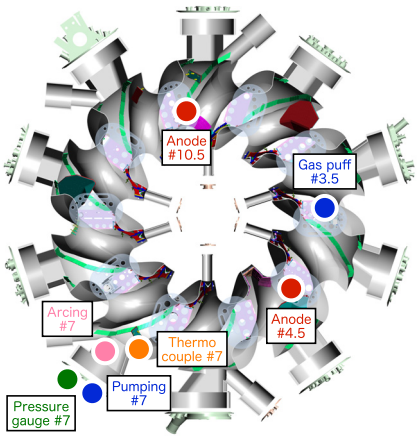

Fig. 2 Top view of the LHD vacuum vessel. Positions of the shutter on which the arc trails occurred, anodes for the GDC, gas puffing, pumping, pressure gauge, and thermocouple are depicted.

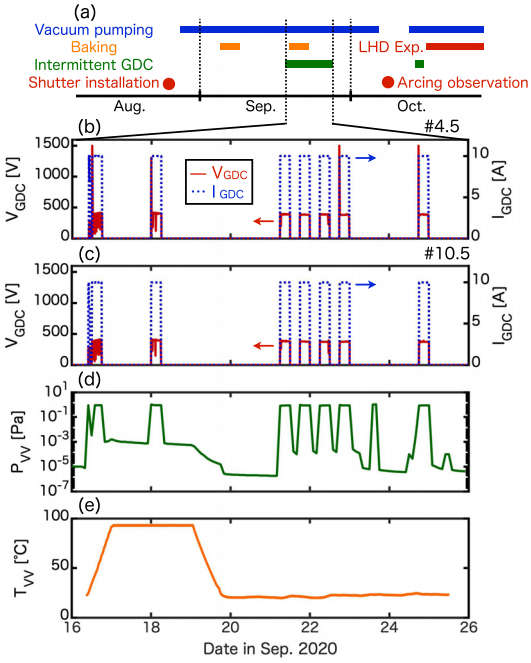

Fig. 3 (a) Machine schedule of LHD before the 22nd experiment campaign. Time evolutions of V_{GDC} and I_{GDC} for the power sources of the anodes at (b) #4.5 and (c) #10.5, (d) P_{VV}, and (e) T_{VV}.

Figure 3 (a) shows the LHD machine schedule before the 22nd campaign. The optical system including the shutter for FIDA diagnostic was installed before the vacuum evacuation. After the wall conditioning by two-time baking and intermittent GDC, the LHD vacuum chamber was vented into the atmosphere. A number of arc trails were observed before the second pumping for the LHD experiment starting from the middle of October in 2020. Figures 3 (b) - (e) show the time evolutions of the voltage, V_{GDC}, and current, I_{GDC}, to maintain the GDC, the pressure, P_{VV}, in LHD chamber and the temperature, T_{VV}, at the first wall in the vicinity of the shutter. In Figs. 3 (b) and (c), V_{GDC} and I_{GDC} are monitored at the power sources of the anodes located at both sections of #4.5 and #10.5. During the GDC, I_{GDC} is kept to be 10 A and V_{GDC} was ~400 V. Although the positive spikes of V_{GDC} were detected a few times at #4.5, the relationship of positive spikes with the arcing ignition is not clear at the moment. P_{VV} is measured by a capacitance manometer during the GDC and by an ionization gauge in the case of P_{VV} below 10^{-2} Pa. The pressure gauges are mounted at the outboard side of #7 in front of the pumping system. The thermocouple embedded on the backside of the first wall nearby the FIDA diagnostic system measures T_{VV}. From 16 Sep. 2020, T_{VV} began to increase for the purpose of baking and maintained a steady-state at ~94°C for 2 days. T_{VV} maintains room temperature except for such a baking phase. The FIDA diagnostic system was exposed to the GDC plasma 8 times. First GDC was conducted by Ne gas for 1 hour. Afterward, H_2 was used for the discharge gas of 6 hours GDC 7 times.

In the present study, we observed the large area with the arcing damage on the Al surface due to the GDC. It should be noted that no other significant arc trails were observed on the surface made of SS in the FIDA diagnostic system and pre-installed materials including SS of first walls. There were some reports indicating the evidence that the LHD GDC initiated arcing on ECH and ECE mirrors [3, 5]. However, the arcing damage observed in the present study shows a larger area than the previous reports during the brief GDC of 43 hours in total. The reason for causing the significant damage might be relevant to the material.

An electron emission process is important to discuss the initiation mechanism of arcing. Thermo-field emission current was theoretically discussed in Ref. [6]. The emitted current is calculated by the electric field, temperature, and work function. The surface roughness, R_a, also an important factor for the field emission, was in the range from 2.5 to 3.0 μm for the flat surfaces of both Al and SS. Regarding the rods, because the R_a has an anisotropy due to the manufacturing process, the comparison is difficult here. At least the flat surfaces of Al and SS could be similar conditions. Further, under the present condition, electric field, determined by the sheath potential and sheath thickness, and temperature are almost the same at Al and SS parts. However, the lower work function of Al, 4.06 - 4.26 eV [7], than that of SS, 4.34 eV [8], enhances the field emission. It is noted that the work function should increase by the absorption of hydrogen and/or oxygen [9] and decrease by the air exposure [10]. These changes of work function due to the gas absorption processes could also have an effect on field emission.

As the conclusion, the current situation of LHD GDC may be on the border that divides the conditions of arcing

ignition between different materials. However, further validation and discussion are necessary from the viewpoints of cohesive energy rule [9], surface roughness, and gas absorption in the future.

This work was supported by NIFS Collaboration Research program (NIFS20KLPP067), NINS program of Promoting Research by Networking among Institutions (01411702), NIFS International Collaboration Research programs (NIFS18KLPR047 and NIFS07KLPH004), LHD project budget (ULRR006, ULRR035, ULRR036, ULRR702, UFEX105).

[1] T. Wauters *et al.*, Plasma Phys. Control. Fusion **62**, 034002 (2020).
[2] T. Akiyama *et al.*, Rev. Sci. Instrum. **78**, 103501 (2007).
[3] D. Hwangbo *et al.*, Plasma Fusion Res. **15**, 2402012 (2020).
[4] Y. Fujiwara *et al.*, Plasma Fusion Res. **14**, 3402129 (2019).
[5] S. Kajita *et al.*, Nucl. Fusion **53**, 053013 (2013).
[6] E.L. Murphy *et al.*, Phys. Rev. **102**, 1464 (1956).
[7] D.R. Lide, 85th ed., *CRC Handbook of Chemistry and Physics, Internet Version 2005*, ⟨http://www.hbcpnetbase.com⟩ (CRC Press, Boca Raton, FL, 2005).
[8] R.G. Wilson, J. Appl. Phys. **37**, 2261 (1966).
[9] A. Anders, *Cathodic Arcs: From Fractal Spots to Energetic Condensation* (New York, USA, Springer, 2008).
[10] Irfan *et al.*, Appl. Phys. Lett. **96**, 243307 (2010).